Journal of GeoEngineering, Vol. 12, No. 4, pp. 147-155, December 2017
http://dx.doi.org/10.6310/jog.2017.12(4).2

SEISMIC GEOTECHNICAL ROBUST DESIGN OF CANTILEVER RETAINING WALL USING RESPONSE SURFACE APPROACH

Parishad Rahbari [1*], Nadarajah Ravichandran [2], and C. Hsein Juang [3]

ABSTRACT

Seismic geotechnical design of retaining walls should consider the uncertainties not only in soil properties such as friction angle of the backfill but also in earthquake load such as peak ground acceleration (PGA). When the uncertainties are incorporated in the design, the robustness which is a measure of sensitivity of a design to uncertain parameters must be considered and evaluated for obtaining suitable design and corresponding construction cost. This paper presents a response surface-based robust geotechnical design approach for cantilever retaining wall subjected to earthquake load. First, the upper and lower bounds of the design variables were determined through dynamic retaining wall design using Mononobe-Okabe method for possible variations in the uncertain parameters. Then, dynamic finite element analyses were performed on a subset of designs by applying El Centro earthquake motions with varying PGA for computing the maximum wall tip deflection which is considered as the serviceability indicator. A response surface for the wall deflection was developed as a function of uncertain and design variables and validated. Finally, a design optimization was performed considering cost and robustness index as the objectives. Two robustness indices, standard deviation of the response and signal to noise ratio were used in this study and the results were compared. The optimization yielded a set of preferred designs, known as Pareto front, and the knee point concept was used to select the final optimal design.

Key words: Uncertainty, dynamic load, retaining wall, response surface, robust design, design optimization.

1. INTRODUCTION

Cantilever retaining walls are known as the simplest and the most commonly-used earth retaining structures in seismic prone areas (Coduto 2001). However, there is no well-established dynamic design procedure available for cantilever retaining walls that considers uncertainties in soil and seismic loading. Therefore, the design of these structures should be carefully performed to ensure that the structure can withstand various earthquake loads under various soil conditions. Generally, the conventional trial-and-error procedure is used to obtain the possible safe designs and the least costly design is selected as the final design. Using this procedure, the geotechnical design of cantilever retaining walls is performed evaluating the stability of wall against sliding, overturning, bearing capacity failure and eccentricity. However, there may be a great number of combinations for design parameters of wall that satisfy the stability requirements. To avoid the time-consuming task of seeking the optimal design from a pool of feasible designs, optimization techniques can be used in the design procedure. Various design optimization approaches have been performed on cantilever retaining walls under static condition in the past in which the objectives were limited to the cost or the weight of wall and the uncertainties in the system were managed implicitly using the concept of factor of safety (FS) (Saribas and Erbatur 1996; Ceranic *et al*. 2001; Yepes *et al*. 2008; Khajehzadeh *et al*. 2008; Camp and Akin 2011). Out of the existing optimization techniques, the genetic algorithm has been found to be useful in managing design optimization of cantilever retaining walls and generally problems with many design variables and complex constraints (Pei and Xia 2012; Juang *et al*. 2013). Coupling the genetic algorithm with finite element analysis, Papazafeiropoulos *et al*. (2013) optimized the cross-sectional area of a cantilever retaining wall subjected to earthquake, assuming constant values for loading and soil properties. Thus, the conventional design of retaining walls optimized to their cost or cross-sectional area often involves the use of deterministic FS-based design where the uncertainties in the system are not incorporated explicitly into the criteria. However, the uncertainties in the properties of soil and loading can lead to uncertainty in the performance of the system (Phoon and Kalhawy 1999). Therefore, a robust design optimization method involving uncertainties in backfill material and seismic loading can be a remarkable contribution towards the conventional design of the cantilever retaining wall. A robust design is referred to the least sensitive design to the unexpected variations in the surrounding uncertainties.

A reliability-based robust design approach is an effective method for considering the uncertainties in optimization process and constraining the system to a specified level of reliability. For example, in the robust design optimization of a cantilever retaining wall performed by Juang *et al*. (2013), the standard deviation of reliability index (as a measure of robustness) and the cost were considered as objectives of optimization and the target reliability was used as the safety constraint. Comparably, Liu *et al*. (2013) used an example of cantilever retaining wall under static loading

Manuscript received May 4, 2017; revised August 8, 2017; accepted September 11, 2017.
[1] Former Graduate Research Assistant (corresponding author), Glenn Department of Civil Engineering, Clemson University, USA (e-mail: prahbar@g.clemson.edu).
[2] Associate Professor, Glenn Department of Civil Engineering, Clemson University, USA.
[3] Professor, Glenn Department of Civil Engineering, Clemson University, USA.

condition to demonstrate a confidence level-based robust design approach. In that study, the confidence level which is the probability of satisfying the target reliability and the cross-sectional area of the wall (as a measure of cost) were deemed as the optimization objectives. Different indices can be defined as robustness measures (*e.g.*, standard deviation of reliability index, standard deviation of probability of failure, and standard deviation of system response), out of which the latter was adopted by Wang *et al*. (2014) in the robust design optimization of braced excavations using genetic algorithm. These previous studies focused mostly on the performance of geotechnical structures under static loading conditions in which the uncertainties are usually limited to soil properties. Nevertheless, while performing seismic designs of the geotechnical structures, the results are highly impacted by the variation in site specific seismic parameters (such as peak ground acceleration, frequency content, and duration of seismic loading) which are difficult to control. To overcome the sensitivity of response to the variation of those seismic parameters, the uncertainties in dynamic loading must be considered along with those in the soil.

In this study, the response surface method was used to avoid simulating a large number of designs which required time-consuming analysis. The response surface method, pioneered in the field of geotechnical engineering by Wong (1985), is the most effective approach for approximating the behavior of geotechnical structures (Massih and Soubra 2008; Guharay and Baidya 2015). In this paper, first the initial seismic geotechnical design procedure of cantilever retaining wall is introduced which is used to offer different design cases. Numerical models were developed for each of these design cases in the finite element software, PLAXIS 2D. Then, the finite element analysis and response surface method, which involves the development of the response function as a representative of response are discussed. Subsequently, the robust design optimization is described in which the geotechnical design of retaining wall is optimized to cost and robustness, meeting the safety requirements. Finally, the optimal final design is sought through a selection procedure, which is described in this paper.

2. RESPONSE SURFACE-BASED ROBUST DESIGN OPTIMIZATION APPROACH

This section describes the major steps of the approach implemented for the geotechnical dynamic design optimization of cantilever retaining wall. The current approach consists of the initial geotechnical design of wall, finite element (FE) simulation, response surface development, and robust design optimization. A flowchart detailing the framework of the study is illustrated in Fig. 1.

2.1 Initial Geotechnical Design of Retaining Wall Subjected to Earthquake Load

In this study, a typical cantilever retaining wall with the height (H) of 6 m and embedded 1 m (at the toe side) into the soil having cohesion (c) of 30 kPa and friction angle (ϕ) of 28° was used to demonstrate the proposed approach. The wall was assumed to have a horizontal sand backfill. As shown in Fig. 2, the geometrical parameters of the wall considered in the study are footing width (X_1), toe length (X_2), footing thickness (X_3), and stem thickness

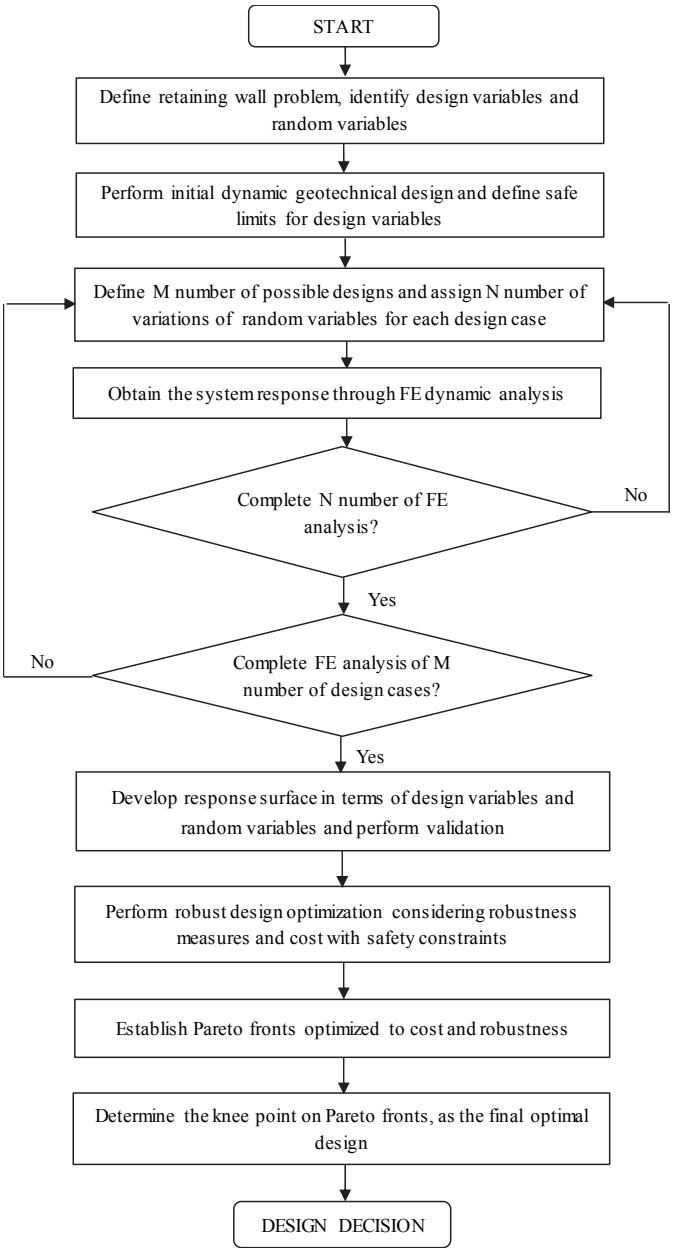

Fig. 1 Flowchart illustrating the framework of the study

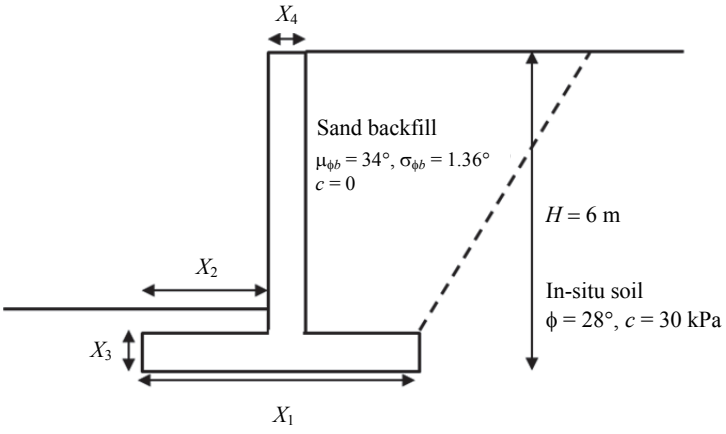

Fig. 2 The sample retaining wall

(X_4). The initial geotechnical dynamic design of wall was conducted checking the wall stability against overturning, sliding, bearing capacity failure and eccentricity considering varying parameters. The dynamic resultant force on the wall was calculated based on pseudo-static analysis using Mononobe- Okabe method (Das 1993) which is the extension of Coulomb theory. The varying parameters of the study can be categorized into two groups: Random variables (*i.e.*, uncertain parameters) and design variables. Out of various properties of soil in the system, the friction angle of the sand backfill (ϕ_b) was chosen as the soil-related random variables in this study. It should be noted that uncertainties in other parameters of sand backfill such as elasticity modulus (stiffness) and properties of in-situ soil can also be considered in future studies. However, in this study the stiffness of sand backfill was varying based on the friction angle of sand backfill which was considered as the soil-related random variable. Another random variable considered in this study along with ϕ_b was coefficient of peak ground acceleration (k_{PGA}) in terms of gravitational acceleration (g = 9.81 m/s^2) of the acceleration-time history of the seismic load. A mean value and a standard deviation of 34° and 1.36° was assumed for ϕ_b with desired range of 30° ~ 38°, regarding that Caltrans utilizes 34° as the default value for friction angle of backfill soil. A mean value (denoted as μ, μ_ϕ, μ_{ϕ_b}) and a standard deviation (denoted as σ, σ_ϕ, σ_{ϕ_b}) of 0.3 and 0.1 was also assumed for k_{PGA} with desired range of 0.1 ~ 0.5, respectively. The statistical properties of k_{PGA} were considered such that the range 0.1 ~ 0.5 covers k_{PGA} range provided in the NCHRP Report 611. On the other hand, X_1, X_2, X_3, and X_4 were assumed as the design variables of the study. Although X_1 is the most effective design variable on meeting the stability requirements of a retaining wall, the factor of safety also varies with a variation in X_2. In addition, X_3 and X_4 both can control the structural design of cantilever retaining wall. The seismic geotechnical designs of the retaining wall for different combinations of the best and worst case scenarios of random variables and design variables were performed. Based on these outcomes, the safe upper and lower limits of the design variables were determined as shown in Table 1. These safe ranges were also finalized by Rahbari (2017) performing safety-based optimizations considering cost and probability of failure of wall for each failure mode (sliding, overturning, bearing capacity failure), which resulted in zero probability of failure.

Based on the ranges determined above, ten different design cases as listed in Table 2 were selected to be implemented in dynamic FE simulations. The geometric properties of design cases are selected in such a way that will cover the full range of variables. For instance, in design case 1 the design variables X_1, X_3, and X_4 are at their lower limit while X_2 is at its upper limit. Similarly, design case 2 was created using the lower limits of all design variables while the upper limits were used in design case 5.

2.2 Dynamic FE Analysis of Retaining Wall

2.2.1 FE Model Generation

The FE models of the subset designs were generated using PLAXIS 2D, which is a FE-based commonly used software in geotechnical engineering and selected for this study (Ravichandran and Huggins 2013; Shrestha *et al*. 2016). It should be noted that the accuracy of the computer simulation results may affect the robust design outcome and several steps must be taken to eliminate/reduce the user controllable errors in the simulations.

Table 1 Limiting values of design variables

Design variable	Suggested range	Range (m)
X_1	$H < X_1 < 1.5H$	$6 < X_1 < 9$
X_2	$0.1 < X_2 < X_1 - X_4$	$0.1 < X_2 < 8.6$
X_3	$H/14 < X_3 < H/10$	$0.42 < X_3 < 0.6$
X_4	$H/14 < X_4 < H/10$	$0.42 < X_4 < 0.6$

Table 2 Design cases of retaining wall selected for finite element simulation

Design case	X_1 (m)	X_2 (m)	X_3 (m)	X_4 (m)
1	6	5.58	0.42	0.42
2	6	0.1	0.42	0.42
3	7.5	3.5	0.51	0.51
4	9	0.1	0.6	0.6
5	9	8.4	0.6	0.6
6	6.5	2	0.55	0.45
7	8	3.75	0.45	0.55
8	7	4	0.48	0.52
9	8.5	3	0.6	0.42
10	6.5	5	0.58	0.58

The steps include evaluation of the simulation domain, the mesh size and the stress-strain behavior of the material, and boundary condition for dynamic analysis. Therefore, a size sensitivity analysis was carried out to determine the size of the simulation domain. For this purpose, the width of the model was varied until the computed response (wall tip displacement-time history in this study) converged to prevent the simulation domain size from affecting the computed results. A similar procedure was followed to obtain a suitable mesh size to eliminate the mesh dependency of the computed results. Specifically, the fineness of the mesh was increased from a coarse mesh until the computed results converged, which in turn yielded simulation domain dimensions (Fig. 3) with a very fine mesh consisting of 1,700 to 2,000 15-node triangular elements.

To apply the regular boundary conditions to the model, the vertical sides of the simulation domain were fixed to prevent horizontal translation and the base of the domain was fixed against both horizontal and vertical movements. The standard earthquake boundary condition suitable for dynamic analysis was applied at the bottom and the vertical sides of the model to ensure that the earthquake waves propagating from the bottom of the model are properly represented. The stress-strain behavior of both the backfill and the in-situ soils were represented by the nonlinear elastoplastic Hardening Soil (HS) material model available in PLAXIS 2D. It is worth noting that linear elastic and Mohr-Coulomb models are usually preferred in static analysis due to determination of few numbers of model parameters but these models might not be suitable for dynamic analysis. Thus, the HS model which takes into account the modulus reduction with strain increase and the small-strain damping, was implemented in this study. The schematic of the stress-strain curve of the HS material model is displayed in Fig. 4, and the values of the key HS model parameters are listed in Table 3 for both in-situ and backfill materials for the selected variations. It should be noted that $q_f(c)$ is the deviatoric stress at failure and E_i is the initial stiffness. These HS soil parameters were adopted based on

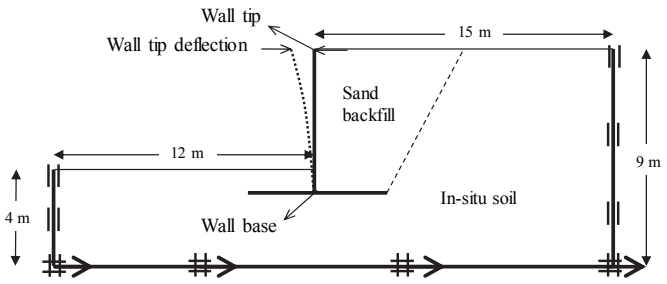

Fig. 3 Schematic of the simulation domain

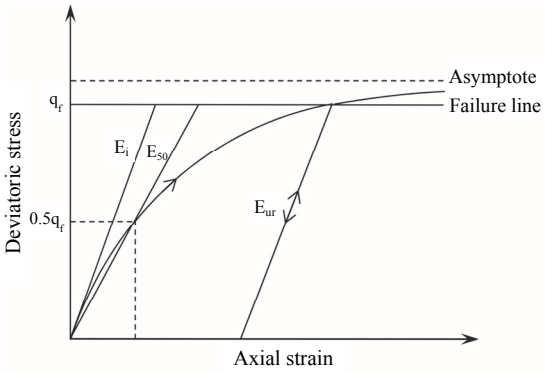

Fig. 4 Stress-strain curve for Hardening Soil model (after Brinkgreve *et al.* 2015)

Table 3 Input parameters for Hardening Soil model

Soil	Variation	ϕ (°)	c (kPa)	E_{50}^{ref} (kPa)	E_{oed}^{ref} (kPa)	E_{ur}^{ref} (kPa)	m	ψ (°)	γ (kN/m^3)
In-situ soil	–	28	30	40150	51154	120450	1	0	18
Sand backfill	μ_ϕ	34	0	47760	60577	143280	0.5	4	18
	$\mu_\phi + 3\sigma_\phi$	38.08	0	62650	77450	187950	0.5	8.08	18
	$\mu_\phi + 2\sigma_\phi$	36.72	0	57800	72325	173400	0.5	6.72	18
	$\mu_\phi + \sigma_\phi$	35.36	0	52250	67307	156750	0.5	5.36	18
	$\mu_\phi - \sigma_\phi$	32.64	0	42100	53846	126300	0.5	2.64	18
	$\mu_\phi - 2\sigma_\phi$	31.28	0	36610	47115	109830	0.5	1.28	18
	$\mu_\phi - 3\sigma_\phi$	29.92	0	32040	40385	96120	0.5	0	18

Note: E_{50}^{ref} = secant stiffness in standard drained triaxial test; E_{oed}^{ref} = tangent stiffness for primary oedometer loading; E_{ur}^{ref} = unloading/reloading stiffness from drained triaxial test; m = the power for stress-level dependency of stiffness; and ψ is the dilatancy angle.

input data needed for PLAXIS 2D (Brinkgreve *et al*. 2015; PLAXIS 2D Manual). The soil stiffness and dilatancy angle were computed based on the friction angle and the randomness in these parameters were considered implicitly in this study. It should be noted that the Young modulus of soil was considered for each friction angle assuming Mohr-Coulomb model. Then, the HS input parameters related to soil stiffness were determined by calibrating the HS model with Mohr-Coulomb model. The HS model parameters can be better calibrated if triaxial test results are available for the soil. It is also worth noting that in the initial phase of PLAXIS 2D modelling the K_0 condition was considered for calculating the initial stresses in the soils. In the next phase after the initial phase, the wall was activated and the K_a (active) condition was considered in models. The wall components (stem and footing) were represented by plate elements and the linear elastic material model was used as the constitutive model of these plates. The properties of the wall for design case 7 are tabulated in Table 4. In addition, the geometrical parameters of the plate wall components were calculated for each design case. Moreover, the accurate modeling requires the consideration of interaction between the wall and the soil. For proper modelling of wall-soil interaction, interfaces that are joint elements were added to wall plates. The roughness of the interaction was modelled by choosing a suitable value for the strength reduction factor (R_{inter}). This factor relates the interface strength (wall friction and adhesion) to the soil strength (friction angle and cohesion). In this study, R_{inter} was assumed to be 0.7. It should also be noted that no gap was considered between wall and the adjacent soil.

Table 4 Properties of the retaining wall structural components for design case 7

Property	Stem	Footing
Linear stiffness, EA (kN/m)	1.25×10^7	1.53×10^7
Flexural stiffness, EI (kN·m^2/m)	2.11×10^5	3.85×10^5
Weight (kN/m/m)	10.60	12.95
Thickness (m)	0.45	0.55
Poisson's ratio	0.12	0.12

2.2.2 Seismic Loading

The first ten seconds of the acceleration-time history of El Centro 1940 earthquake, as shown in Fig. 5(a), was adopted for dynamic FE simulations. This record, with the PGA of approximately 0.3 g, is often used as the reference earthquake motion in the seismic design and analysis of current structures and geotechnical systems. To apply the variations of k_{PGA} in the FE analyses, the El Centro 1940 acceleration-time history was scaled to PGA of 0.1 g, 0.2 g, 0.4 g, and 0.5 g and used as the ground motion. The sample acceleration-time history with PGA of 0.1 g is shown in Fig. 5(b). As mentioned earlier, mean and standard deviation of k_{PGA} were assumed to be 0.3 and 0.1, respectively in the robust design optimization procedure. It should be noted that in this study the uncertainty in seismic loading was limited to PGA of the input ground motion (El Centro 1940), and considering sets of different ground motions is recommended for future studies to take the frequency content, duration and other amplitude parameters of seismic loading into account as random variables.

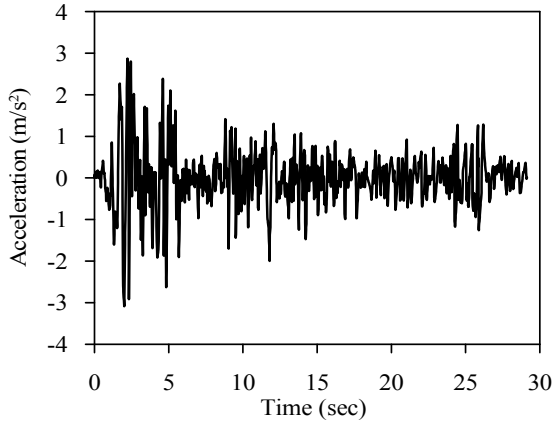

(a) PGA = 0.3 g

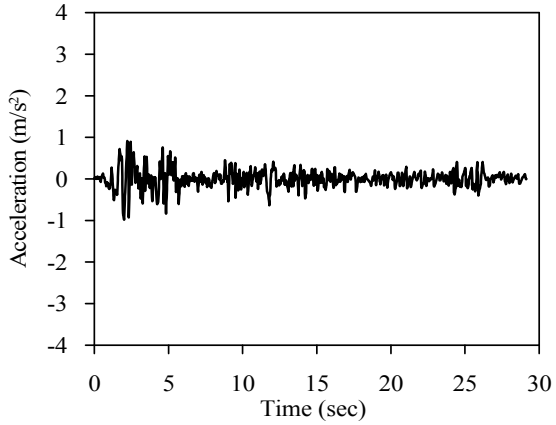

(b) PGA = 0.1 g

Fig. 5 El Centro acceleration-time history

2.2.3 Results

The primary outcomes of PLAXIS 2D models are the wall displacement, shear force, and the bending moment. Using the wall displacement output, the wall tip deflection-time history was obtained by subtracting the wall base displacement-time history from wall tip displacement-time history. The sample wall tip deflection-time histories for design cases 2 and 7 are shown in Fig. 6. Then the maximum wall tip deflection (d_{max}) was determined from wall tip deflection-time history and considered as the response of concern in this study. It should be noted that the wall tip deflection controls the safety and stability of the system and is also easily measured while shear force and bending moment can be easily manipulated via reinforcement in the structural design. The representative of input variables and response for one design case is tabulated in Table 5 as a sample simulation table and was applied to all selected design cases. For each design case, total 11 FE analyses were performed: One analysis for mean values of random variables, six analyses for considering variations in friction angle and four analyses for considering variations in PGA.

2.3 Response Surface Development

Using results obtained from the FE dynamic analysis, the response surface method was then implemented to model the system response. The response surface was developed via regression analysis between the input variables (ϕ, k_{PGA}, X_1, X_2, X_3, and X_4), and the response (d_{max}). Among the models commonly used in the response surface method, the logarithmic regression model, expressed in Eq. (1), which fitted the data points reasonably well, was used in this study.

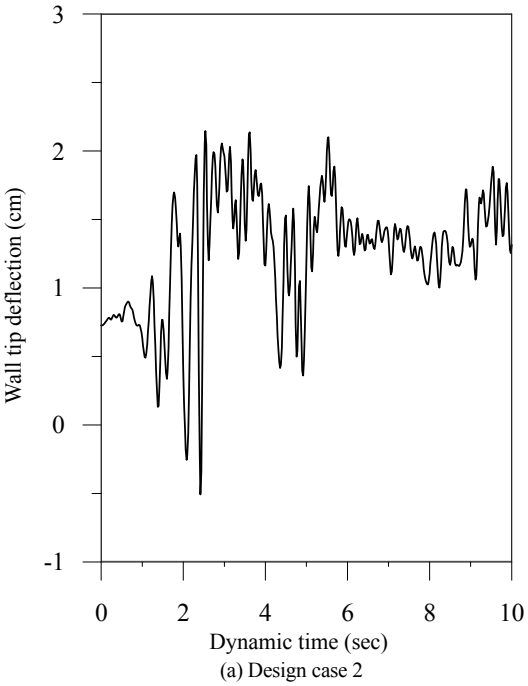

(a) Design case 2

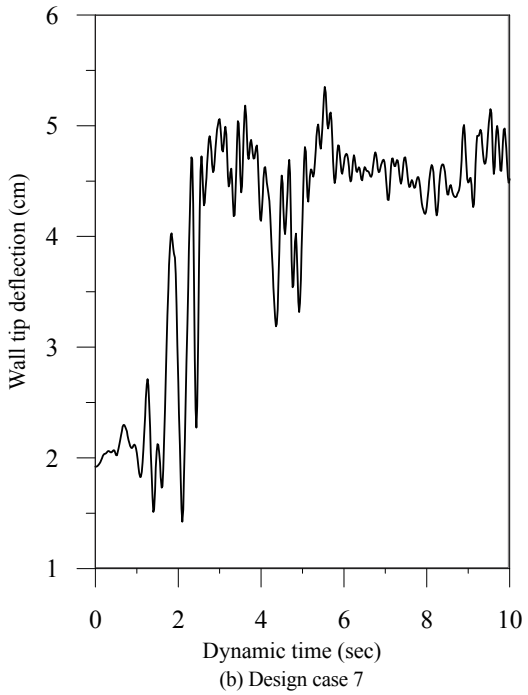

(b) Design case 7

Fig. 6 Wall tip deflection-time history

Table 5 Sample simulation table for one design case

Design variables				Random variables		Response
X_1	X_2	X_3	X_4	ϕ	k_{PGA}	d_{max}
Values of the design case				μ	μ	d_1
				$\mu + 3\sigma$	μ	d_2
				$\mu + 2\sigma$	μ	d_3
				$\mu + \sigma$	μ	d_4
				$\mu - \sigma$	μ	d_5
				$\mu - 2\sigma$	μ	d_6
				$\mu - 3\sigma$	μ	d_7
				μ	$\mu + 2\sigma$	d_8
				μ	$\mu + \sigma$	d_9
				μ	$\mu - \sigma$	d_{10}
				μ	$\mu - 2\sigma$	d_{11}

$$y = \exp\left(b_0 + \sum_{i=1}^{n} b_i \ln(x_i) \right) \quad (1)$$

where y and x_i denote the response and input variables respectively and b_0 and b_i are the coefficients. Using the aforementioned model and determining the model coefficients, the response surface of the study was constructed as displayed below with R^2 (coefficient of determination) equal to 0.93.

$$d_{\max} = \exp\left(\begin{array}{l} 1.543 - 0.717 \ln(\phi) + 0.419 \ln(k_{PGA}) + \\ 0.389 \ln(X_1) - 0.169 \ln(X_2) - 1.735 \ln(X_3) - 0.62 \ln(X_4) \end{array} \right) \quad (2)$$

The response surface presented in Eq. 2, as the serviceability indicator of the cantilever retaining wall, represents the system response in terms of maximum wall tip deflection considering wall geometry and uncertainties in backfill and dynamic loading. In other words, approximate behavior of retaining wall with sand backfill, specific height, and specific in-situ soil properties can be predicted by considering uncertainties of the system. This methodology obviates the usual need for thousands of time-consuming analyses, thus greatly accelerating the process. However, performing the design optimization based on the established response surface is first predicated on evaluating the validity and rating the performance of the response surface.

To conduct the validation procedure, twenty random design sets combined with twenty random values for random variables within their specified ranges were generated and modeled in PLAXIS 2D. Subsequent results compared with those obtained from the response surface, as shown in Fig. 7, show that the points are closely adjacent to the line $y = x$. and a close agreement between the two sets of results is observed.

However, this visual method of validation may be insufficient for finalizing the response surface. To assess the accuracy of the regression in a quantitative manner, additional indicators may need to be applied. Moriasi *et al*. (2007) recommended three quantitative statistics for evaluating the simulation results per the observed results: The Nash-Sutcliffe efficiency (NSE), the percent bias (PBIAS), and the ratio of the root mean square error to the standard deviation of measured data (RSR) described respectively in Eqs. (3), (4), and (5).

$$\mathrm{NSE} = 1 - \left[\frac{\sum_{i=1}^{n} (Y_i^{obs} - Y_i^{sim})^2}{\sum_{i=1}^{n} (Y_i^{obs} - Y_i^{mean})^2} \right] \quad (3)$$

$$\mathrm{PBIAS} = \left[\frac{\sum_{i=1}^{n} (Y_i^{obs} - Y_i^{sim}) \times 100}{\sum_{i=1}^{n} Y_i^{obs}} \right] \quad (4)$$

$$\mathrm{RSR} = \frac{\left[\sqrt{\sum_{i=1}^{n} (Y_i^{obs} - Y_i^{sim})^2} \right]}{\left[\sqrt{\sum_{i=1}^{n} (Y_i^{obs} - Y_i^{mean})^2} \right]} \quad (5)$$

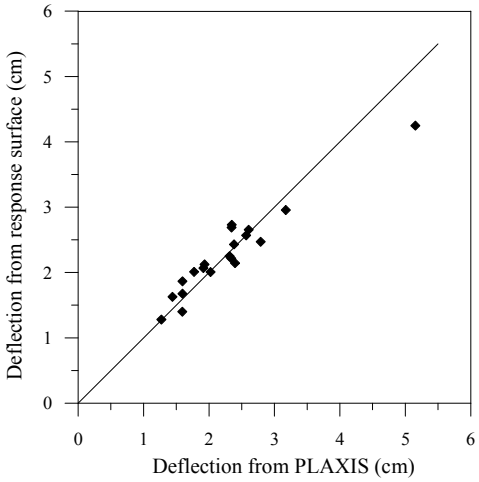

Fig. 7 Graph of wall tip deflection obtained by PLAXIS 2D and response surface

where Y_i^{obs} is the observation, Y_i^{sim} is the simulated value and Y_i^{mean} is the mean of observed data. Here, the response resulted from PLAXIS 2D model and from response surface are considered as Y_i^{obs} and Y_i^{sim}, respectively. These validation statistics were then computed and evaluated based on Table 6 to estimate the precision of the obtained values from the response surface. The statistics values shown in Table 7 demonstrate that the performance of response surface ranged from good to very good and the overall performance can be described conservatively as good. In sum, the combination of both visual technique and quantitative statistics were utilized to validate the response surface and ensure its reliability for use in the design optimization process.

2.4 Design Optimization of Retaining Wall

To first acquire a set of preferred designs and then a single optimal design, an optimization algorithm was used to define, implement and then minimize a set of objective functions. Therefore, the authors applied NSGA-II (Non-dominated Sorting Genetic Algorithm), developed by Deb *et al*. (2002), for the design optimization of the retaining wall. In this study, the design optimization involves minimizing the cost (material usage) of the wall and maximizing the robustness of the system. Concurrent with ensuring that the optimization is both robust and economical, constraints are also used to meet the safety requirements of defined target reliability, allowable wall tip deflection, and toe length limit. In this study, two robustness indices suitable for adaptation into the robust design procedure were standard deviation of response and signal-to-noise ratio of the system. Here, maximizing the robustness of the system means desensitizing the response of the system to various uncertainties, by either minimizing the standard deviation of the response or by maximizing the signal-to-noise ratio of the system. Computing these robustness indices requires defining the performance function of the system, as expressed in Eq. 6, using the response surface discussed in previous section, and considering an allowable deflection for the wall tip,

$$g(\theta, X) = d_{all} - d(\theta, X) \quad (6)$$

Table 6 Performance ratings for recommended statistics (after Moriasi *et al.* 2007)

Performance rating	RSR	NSE	PBIAS[a]
Very good	0 ~ 0.5	0.75 ~ 1	< ±15
Good	0.5 ~ 0.6	0.65 ~ 0.75	±15 ~ ±30
Satisfactory	0.6 ~ 0.7	0.5 ~ 0.65	±30 ~ ±55
Unsatisfactory	> 0.7	< 0.5	> ±55

[a] Ranges were problem-dependent and the average one is considered here

Table 7 Response surface validity

Statistics	Value	Performance
RSR	0.347	Very good
NSE	0.653	Good
PBIAS	0.309	Very good

where θ and X are the respective symbols of the random and design variables; $g(\theta, X)$ = performance function, d_{all} = the allowable wall tip deflection, and $d(\theta, X)$ = the response surface of $d_{\max}$. In this study, the allowable maximum wall tip deflection was assumed to be 3 cm which is equal to 0.5% of the wall height (6 m). This value of deflection-to-height ratio (d/H %) was selected based on past studies in which the range of 0 ~ 0.5 % was considered for ratio, for example, for evaluating the effect of PGA on the ratio (Mikola and Sitar 2013), and evaluating the ratio for variation of earthquake pressure force on wall as discussed in Supplementary Guidance on seismic design of retaining structures in Greater Christchurch (2004). The value of allowable maximum wall tip deflection also varies with project/location. Moreover, standard deviation of the response (SD) can be computed using First Order Second Moment (FOSM) method, as expressed in Eq. 7, assuming there is no correlation between ϕ and k_{PGA}.

$$\mathrm{SD} = \sigma\big(d(\theta, X)\big) = \sqrt{\left(\frac{\partial d(\theta, X)}{\partial \phi}\right)^2 \sigma_\phi^2 + \left(\frac{\partial d(\theta, X)}{\partial k_{PGA}}\right)^2 \sigma_{k_{PGA}}^2} \tag{7}$$

Another measure of design robustness that has been used in quality engineering is the signal-to-noise ratio (SNR). Maximizing the SNR of a system leads to identify the most robust design from a pool of designs. This robustness measure is defined as following (Phadke 1995):

$$\mathrm{SNR} = 10 \log_{10}\left(\frac{\mu^2\big(g(\theta, X)\big)}{\sigma^2\big(g(\theta, X)\big)}\right) \tag{8}$$

where $\sigma(g(\theta, X))$ = the standard deviation of the performance function (numerically equal to the SD), and $\mu(g(\theta, X))$ = the mean value of performance function obtained using Eq. (9),

$$\mu\big(g(\theta, X)\big) = g(\mu_\theta, X) \tag{9}$$

where μ_θ is the mean value of random variables.

In this study, the robust design optimization, was performed twice first using SD as first objective and then using SNR while keeping cost as the second objective in both optimizations. It should be noted that 1/SNR was used as the objective so that by minimizing 1/SNR the designs of the higher SNR are obtained. For cost (the second objective) the volume of the retaining wall per unit length was adopted in optimization setting. The objective functions of the study are summarized as below:

$$\text{Objective function 1}: y_1 = \mathrm{SD} \ \text{ or } \ y_1 = 1/\mathrm{SNR} \tag{10}$$

$$\begin{aligned}\text{Objective function 2}: y_2 &= \mathrm{Cost}(m^3/m) \\ &= X_1 X_3 + (H - X_3) X_4\end{aligned} \tag{11}$$

To manage the screened designs in the design optimization process, a target reliability index (β_t) equal to 3 was considered as constraint to prevent inclusion of designs of lower reliability into the set of suitable designs. The mean value and standard deviation of performance function as shown in Eq. (12) was then used to compute the reliability index of system (β), which is expressed as:

$$\beta = \frac{\mu\big(g(\theta, X)\big)}{\sigma\big(g(\theta, X)\big)} \tag{12}$$

It is also possible to constrain the optimization setting by limiting the toe width to approximately half of the footing width; this constraint is considered as a justification for typical engineering preferences. Generally, depending on the properties on both sides of the retaining wall and wall ownership, the extension of the toe can be limited. For example, if the upstream neighbor is assumed to be the wall owner and responsible for all wall repairs, the downstream neighbor will be responsible for all toe repairs (as the wall toe is located within the downstream property), and will not face an unacceptable charge if the constraint is applied to the wall.

Based on the design optimization setting in this study as shown in Fig. 8, a set of preferred designs were obtained and displayed in a curve, also known as a Pareto front, from which the optimum final design can be extracted. The Pareto fronts established through the NSGA-II algorithm consist of a number of data points, each representing a suitable design case, with values of computed objectives.

3. DESIGN OPTIMIZATION RESULTS AND DISCUSSION

Following the response surface-based robust design optimization in this study, the designs within the safe design domain were screened based on the optimization settings and demonstrated collectively in Pareto front. A clear trade-off relationship between the cost and the robustness index can be inferred from the obtained Pareto front as shown in Fig. 9. In other words, either decreasing the standard deviation or increasing the SNR which desensitized the system towards uncertainties in turn yielded retaining walls that had a greater volume per unit length, which were represented in a more costly design. This incompatibility in the relationship between two objectives required an investigation of the main characteristics of the established Pareto front, particularly the knee point concept to determine the best trade-off solution, or final optimal design.

Find: Design parameters $X = \{X_1, X_2, X_3, X_4\}$

Objectives: Maximizing design robustness:
(i) minimizing SD
(ii) maximizing SNR

Minimizing Cost

Subject to: X ∈ safe design range
$\beta > \beta_T$

Fig. 8 Robust design optimization setting of the study

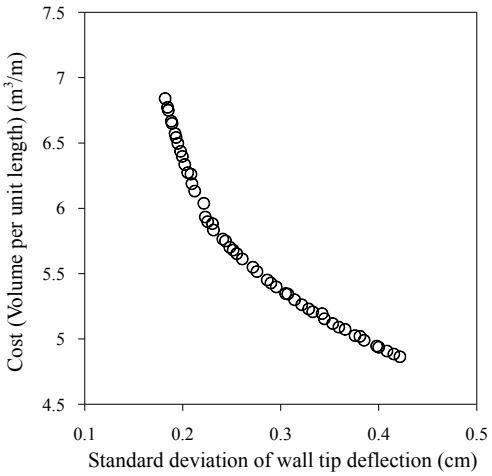

Fig. 9 Pareto front optimized to both cost and robustness (SD)

As clearly indicated in Fig. 9, the Pareto front based on case (i) in optimization setting, the variation of the standard deviation of wall tip deflection as a representative of variation of system response was between 0.1 cm and 0.4 cm. Also, the volume per unit length, which simply represents the cost of materials used in the construction of the wall, decreased from approximately 7 m^3/m to 4.5 m^3/m with an increase in the standard deviation. Each point in the following set of Pareto fronts is a demonstration of a design case with its specific value of cost (volume per unit length) and a standard deviation of wall tip deflection. The optimal design is assumed as a point at which both objectives remain at the minimum condition.

A second Pareto front, as shown in Fig. 10, was also established based on case (ii) of the optimization setting which was examination of the 1/SNR as another robustness measure for the design optimization. Similar to the first case, the results show a trade-off relationship in which a decrease in the volume of wall causes a corresponding increase in the 1/SNR and reduction in SNR and thus in robustness.

In order to determine the optimal design with respect to cost and robustness, the normal boundary intersection (NBI) (Das and Dennis 1998) approach was used to compute the knee points on the two Pareto fronts. As shown in Fig. 11, for each point of the Pareto front, the distance from the boundary line, which connects the highest point of the Pareto front to the lowest point, is computed in the normalized space of Pareto front. Then, the point with maximum distance from the boundary line is sought and selected as the knee point which corresponds to the optimal design of the study.

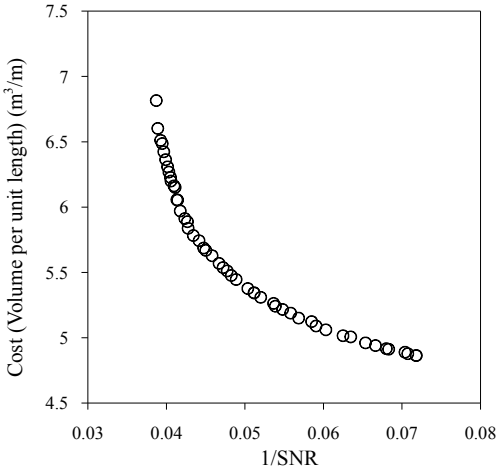

Fig. 10 Pareto front optimized to cost and robustness (1/SNR)

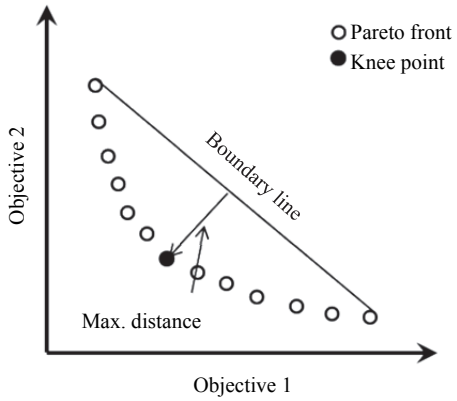

Fig. 11 Normal boundary intersection approach

The results of final optimal design using both robustness measures are summarized in Table 8, which holds the design parameter values of the retaining wall obtained from the properties of the knee points of both Pareto fronts. The consistency of both sets of results can be interpreted as different robustness measures yielded similar design sets and also as evidence of the appropriateness of the developed response surface. The obtained design parameters from knee points indicate that the final optimal design, which is identified as the most cost-efficient and the most robust design simultaneously, includes minimum footing width, maximum footing thickness, and minimum stem thickness based on the limiting values of the design range.

Both Pareto fronts can also be used to obtain the final design based upon the engineering preferences and available sources (*e.g.,* a specific budget). These provide an option for designers to choose a desired level of robustness for determining the final design that corresponds to a specific level of optimization. Moreover, the expertise of engineer, can be applied to inform the addition of constraints to the optimization setting. These features that increase the flexibility of the current methodology are advantageous in ensuring the robust design optimization.

When comparing the Pareto front with a conventional design, the design with the least cost, which corresponds to the least robust design on the Pareto front, is considered as the final design in conventional practices. In the current approach, safety is the common requirement shared between the robust design and conventional designs, which is applied in the initial design step and serves as an initial constraint in the design optimization.

Table 8 Summary of final optimal designs properties

Robustness measure	X_1 (m)	X_2 (m)	X_3 (m)	X_4 (m)
SD	6	2.96	0.59	0.42
SNR	6	2.97	0.54	0.42

4. CONCLUSIONS

In this paper, the authors presented a framework of response surface-based robust geotechnical design of a retaining wall backfilled with sand subjected to earthquake load. The adopted approach which is conducted through the coupling of FE dynamic analysis and response surface development linked to bi-objective optimization considers safety, robustness, and cost simultaneously in the geotechnical design of a retaining wall. The robustness of the design was satisfied by minimizing the standard deviation of response and maximizing the SNR in two attempts. The safety of design was ensured by performing stability analysis of the initial design and then defining target reliability index and allowable wall tip deflection. It should also be noted that the sources of system uncertainties, mainly identified in backfill material and in seismic loading, were considered as random variables to reduce the variation in system response along with carefully adjusting the design variables.

This approach can be introduced as a beneficial tool for the geotechnical dynamic design of retaining structures with which designers may work with more efficient designs to prevent an overdesign because of safety satisfactions or an under-design, which results from cost concerns. Moreover, the concept of knee point can be utilized based on the obtained Pareto fronts from design bi-objective optimizations to aid in the selection of the final optimal design from a series of safe designs.

ACKNOWLEDGMENTS

This research was supported by Glenn Department of Civil Engineering, Clemson University.

REFERENCES

Anderson, D.G., Martin, G.R., Lam, I.P., and Wang, J.N. (2008). *Seismic Design and Analysis of Retaining Walls, Buried Structures, Slopes and Embankments*. NCHRP Report 611. Transportation Research Board, National Cooperative Highway Research Program.

Basudhar, P.K., Lakshman, B., and Dey, A. (2006). "Optimal cost design of cantilever retaining walls." *Indian Geotechnical Conference, IGC*, Chennai, 14–16.

Brinkgreve, R.B.J., Kumarswamy, S., and Swolfs, W.M. (2015). *PLAXIS 2D Manual*. PLAXIS bv, the Netherlands.

Camp, C.V. and Akin, A. (2011). "Design of retaining walls using big bang-big crunch optimization." *Journal of Structural Engineering*, ASCE, **138**(3), 438–448.

Caltrans. (2014). *Memo to Designers — Existing Bridges*. California Department of Transportation, 9-5.

Ceranic, B., Fryer, C., and Baines, R.W. (2001). "An application of simulated annealing to the optimum design of reinforced concrete retaining structures." *Computers and Structures*, **79**(17), 1569–1581.

Coduto, D.P. (2001). *Foundation Design: Principles and Practices*, Prentice Hall.

Das, B.M. (1993). *Principles of Geotechnical Engineering*, 3rd Ed., PWS Publishing, Boston.

Das, I. and Dennis, J.E. (1998). "Normal-boundary intersection: A new method for generating the Pareto surface in nonlinear multicriteria optimization problems." *SIAM Journal on Optimization*, **8**(3), 631–657.

Deb, K., Pratap, A., and Agarwal, S. (2002). "A fast and elitist multiobjective genetic algorithm NSGA-II." *Evolutionary Computation*, **6**(2), 182–197.

Guharay, A. and Baidya, D.K. (2015). "Reliability-based analysis of cantilever sheet pile walls backfilled with different soil types using the finite-element approach." *International Journal of Geomechanics*, ASCE, **15**(6), 06015001.

Juang, C.H., Liu, Z., and Atamturktur, H.S. (2013). "Reliability-based robust geotechnical design of retaining walls." *Sound Geotechnical Research to Practice*, 514–524.

Khajehzadeh, M., Taha, M.R., El-Shafie, A., and Eslami, M. (2010). "Economic design of retaining wall using particle swarm optimization with passive congregation." *Australian Journal of Basic and Applied Sciences*, **4**(11), 5500–5507.

Liu, Z., Juang, C.H., and Atamturktur, S. (2013). "Confidence level-based robust design of cantilever retaining walls in sand." *Computers and Geotechnics*, **52**, 16–27.

Ministry of Business, Innovation & Employment (2014). *Guidance on the Seismic Design of Retaining Structures for Residential Sites in Greater Christchurch. Supplementary Guidance*. Version 2.

Mikola, R.G. and Sitar, N. (2013). *Seismic Earth Pressures on Retaining Structures in Cohesionless Soil*. Report No. UCB GT 13-01, University of California, Berkeley.

Moriasi, D.N., Arnold, J.G., van Liew, M.W., Bingner, R.L., Harmel, R.D., and Veith, T.L. (2007). "Model evaluation guidelines for systematic quantification of accuracy in watershed simulations." *Transactions of the ASABE*, **50**(3), 885–900.

Papazafeiropoulos, G., Plevris, V., and Papadrakakis, M. (2013). "Optimum design of cantilever walls retaining linear elastic backfill by use of genetic algorithm." *Proc., 4th ECCOMAS Thematic Conference on Computational Methods in Structural Dynamics and Earthquake Engineering*, Greece.

Pei, Y. and Xia, Y. (2012). "Design of reinforced cantilever retaining walls using heuristic optimization algorithms." *Procedia Earth and Planetary Science*, **5**, 32–36.

Phadke, M.S. (1995). *Quality Engineering Using Robust Design*. Prentice Hall PTR.

Phoon, K.K. and Kulhawy, F.H. (1999). "Evaluation of geotechnical property variability." *Canadian Geotechnical Journal*, **36**(4), 625–639.

Rahbari, P. (2017). "Robust geotechnical design optimization of retaining walls and levees." Ph.D. Dissertation, Department of Civil Engineering, *Clemson University, USA*.

Ravichandran, N. and Huggins, E.L. (2003), "Seismic response of gravity-cantilever retaining wall backfilled with shredded tire." *Geotechnical Engineering*, SEAGS & AGSSEA, **44**(3), 14–24.

Saribas, A. and Erbatur, F. (1996). "Optimization and sensitivity of retaining structures." *Journal of Geotechnical Engineering*, ASCE, **122**(8), 649–656.

Shrestha, S., Ravichandran, N., Raveendra, M., and Attenhofer, J.A. (2016). "Design and analysis of retaining wall backfilled with shredded tire and subjected to earthquake shaking." *Soil Dynamics and Earthquake Engineering*, **90**, 227–239.

Wang, L., Juang, C.H., Atamturktur, S., Gong, W., Khoshnevisan, S., and Hsieh, H.S. (2014). "Optimization of design of supported excavations in multi-layer strata." *Journal of GeoEngineering*, TGS, **9**(1), 1–12.

Wong, F.S. (1985). "Slope reliability and response surface method." *Journal of Geotechnical Engineering*, ASCE, **111**(1), 32–53.

Yepes, V., Alcala, J., Perea, C., and González-Vidosa, F. (2008). "A parametric study of optimum earth-retaining walls by simulated annealing." *Engineering Structures*, **30**(3), 821–830.

Youssef Abdel Massih, D.S. and Soubra, A.H. (2008). "Reliability-based analysis of strip footings using response surface methodology." *International Journal of Geomechanics*, ASCE, **8**(2), 134–143.